Ultrafast polychromatic ionization of dielectric solids

P. Jürgens[a], M. Jupé[b], M. Gyamfi[b], and D. Ristau[b,c]

[a]Max Born Institute for Nonlinear Optics and Short Pulse Spectroscopy, Max-Born-Strasse 2A, 12489 Berlin, Germany
[b]Laser Zentrum Hannover, Hollerithallee 8, 30149 Hannover, Germany
[c]Institut für Quantenoptik, Leibniz Universität Hannover, Welfengarten 1, 30167 Hannover, Germany

ABSTRACT

The modeling of the laser-induced damage processes can be divided into thermal and electronic processes. Especially, electronic damage seems to be well understood. In corresponding models, the damage threshold is linked to the excitation of valence electrons into the conduction band, and often the damage is obtained if a critical density of free electrons is exceeded. For the modeling of the electronic excitation, rate equation models are applied which can vary in the different terms representing different excitation channels. According to the current state of the art, photoionization and avalanche ionization contribute the major part to the ionization process, and consequently the determination of laser-induced damage thresholds is based on the calculation of the respective terms. For the theoretical description of both, well established models are available. For the quantitative calculation of the photoionization, the Keldysh theory is used most frequently, and for the avalanche processes the Drude theory is often applied. Both, Drude and Keldysh theory calculations depend on the laser frequency and use a monochromatic approach. For most applications the monochromatic description matches very well with the experimental findings, but in the range of few-cycle pulses the necessary broadening of the laser emission spectrum leads to high uncertainty for the calculation.
In this paper, a novel polychromatic approach is presented including photo- and avalanche ionization as well as the critical electron density. The simulation combines different ionization channels in a Monte-Carlo procedure according to the frequency distribution of the spectrum. The resulting influence on the wavelength and material dependency is discussed in detail for various pulse shapes and pulse durations. The main focus of the investigation is concentrated on the specific characteristics in the dispersion and material dependency of the laser-induced damage threshold respecting the polychromatic characteristics of the ultra-short pulse (USP) laser damage.

Keywords: Ultrafast, polychromatic, ionization, laser-induced damage

1. INTRODUCTION

Theoretical approaches for laser matter interaction in the regime of USP have been studied extensively in the past.[1–3] Progress in modeling nonlinear ionization processes in dielectric materials opened up the possibility to determine the behavior of wide band gap dielectrics irradiated by USP in detail.[4,5] State of the art simulations match experimental results very well in the case of pulse durations of a few hundred femtoseconds.[6,7] The development of laser systems with ever decreasing pulse durations drives the demand for a theory that describes fundamental processes in laser matter interaction down to the single-optical-cycle limit.
The majority of the existing models are based on the theory for photoionization published by Keldysh in 1965[8] and on the Drude-Model to include avalanche ionization.[9] The main limitation of these models is given by the monochromatic structure of the photoionization rate and the available models for the avalanche ionization mechanism. As a consequence, the spectral width of the laser pulses is neglected in the calculations. This might lead to a miscalculation of the ionization rate, because a broad spectrum of the laser pulse opens up various further excitation channels for a multiphoton ionization process than just considering one wavelength.
Recent publications have discussed the influence of propagation effects on the change of the central wavelength

Further author information: (Send correspondence to P.J.)
P.J.: E-mail: juergens@mbi-berlin.de, Telephone: +49 (0)30 63 92 12 38

Laser-Induced Damage in Optical Materials 2016, edited by Gregory J. Exarhos, Vitaly E. Gruzdev, Joseph A. Menapace, Detlev Ristau, MJ Soileau, Proc. of SPIE Vol. 10014, 100141C
 · doi: 10.1117/12.2244833

and the subsequent modification of the ionization rate.[4] Further investigations were focused on the influence of the instantaneous intensity as the standard Keldysh formalism only considers the cycle averaged intensity.[10] Nevertheless, a comprehensive model, that considers the influence of the spectral width of USP during ionization of solids, is still not available.
In this paper we present a probabilistic model to implement the spectrum of the laser pulse into the calculation of the ionization rate. Additionally, results for the theoretical laser-induced damage threshold (LIDT) in dependence of the central wavelength are presented for different temporal pulse shapes and dielectric materials.

2. THEORY AND MODELING

The spectral width of USP directly follows from the time-frequency uncertainty relation

$$\Delta\nu\,\tau_p \geq c_{\mathrm{TBP}}\,, \tag{1}$$

where $\Delta\nu$ represents the full-width-half-maximum (FWHM) frequency bandwidth and τ_p the FWHM pulse duration of the laser pulse. Equality in equation 1 is only valid for the case of bandwidth limited pulses. The time-bandwidth product c_{TBP} is a constant which only depends on the temporal intensity profile of the pulse. For a laser pulse of central wavelength λ_0 the spectral width in terms of wavelengths $\Delta\lambda$ is given by

$$\Delta\lambda \geq \frac{\lambda_0^2}{\tau_p}\frac{c_{\mathrm{TBP}}}{c}\,, \tag{2}$$

with speed of light in vacuum c. Equation 2 implies that the spectral width scales quadratically with the central wavelength and linarly with the inverse pulse duration. Common temporal pulse shapes are displayed in figure 1(a) next to the spectral intensity distributions obtained by fourier transformation in figure 1(b). The corresponding spectral width in dependence of the pulse duration for central wavelengths of 400 nm and 800 nm according to equation 2 is displayed in figure 1(c). The related equations for temporal and spectral intensity profiles are given in table 1 together with the particular time-bandwidth product.

In accordance with equation 2 the spectral width is significantly higher for a longer central wavelength and

Table 1. Mathematical description and corresponding time-bandwidth product of different temporal pulse shapes

Pulse shape	Temporal Intensity Profile	Spectral Intensity Distribution	c_{TBP}
Rectangular	1 for $\lvert\frac{t}{\tau_p}\rvert \leq 1, 0$ else	$\mathrm{sinc}^2[(\omega-\omega_0)\tau_p]$	0.443
Lorentzian	$\left(1+\frac{4}{1+\sqrt{2}}(\frac{t}{\tau_p})^2\right)^{-2}$	$\exp[-\sqrt{1+\sqrt{2}}\tau_p\lvert\omega-\omega_0\rvert]$	0.142
Hyperbolic Secant	$\mathrm{sech}^2[2\log(1+\sqrt{2})\frac{t}{\tau_p}]$	$\mathrm{sech}^2[\frac{\pi\tau_p(\omega-\omega_0)}{4\log(1+\sqrt{2})}]$	0.315
Gaussian	$\exp[-4\log(2)(\frac{t}{\tau_p})^2]$	$\exp[-\frac{\tau_p^2(\omega-\omega_0)^2}{4\log(2)}]$	0.441

increases with decreasing pulse duration. Additionally, the spectral width for gaussian and rectangular pulses is nearly identical because of their similar c_{TBP}-factors. For lorentzian shaped pulses the spectral width is significantly smaller than for other shapes as predicted by the time-bandwidth product.

2.1 Plasma formation in dielectric materials

Plasma formation in dielectric materials exposed to USP is often modeled on the basis of a single rate equation describing the conduction band electron density $\rho(t)$ of the irradiated material.[1,11] The conduction band electrons

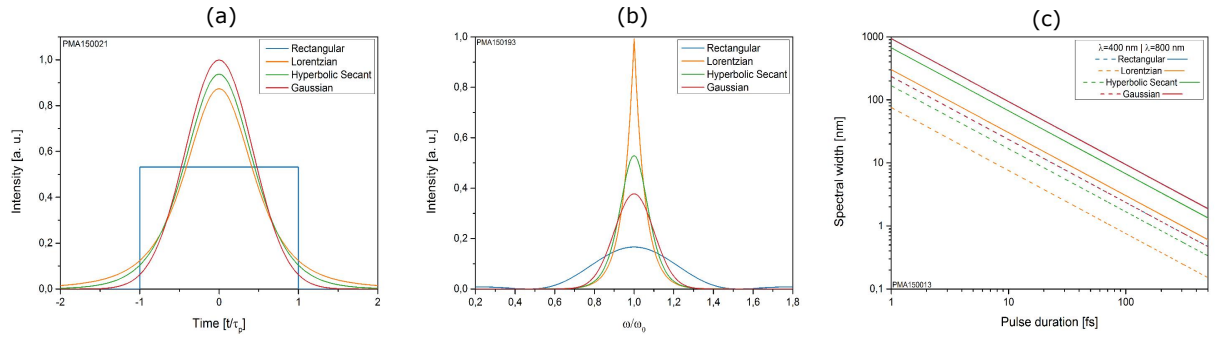

Figure 1. (a) temporal pulse shapes as given in table 1, (b) corresponding spectra of given temporal shapes with a pulse duration of $\tau_p = 5\,\mathrm{fs}$, (c) spectral width in dependence of pulse duration according to equation 2 for a central wavelength of 400 and 800 nm

can thereby be excited either by photoionization (PI) or avalanche ionization (AI). In combination with a relaxation term to approximate an exponential decay of excited carriers into valence or interband states with a characteristic relaxation time τ_r the rate equation reads

$$\frac{\partial \rho(t)}{\partial t} = W_{PI}(I(t),\lambda) + W_{AI}(I(t),\rho(t),\lambda) - \frac{\rho(t)}{\tau_r} \tag{3}$$

In this equation only the third term on the right hand side does not explicitly depend on the wavelength. Both the PI and the AI rate strongly depend on the laser frequency. Thus, these two terms have to be modified to include the spectral width of the USP in the simulation of laser matter interaction. The PI rate W_{PI} for a single frequency is calculated using the traditional Keldysh-formalism[8]

$$W_{PI} = \frac{2\omega_0 Q}{9\pi}\left(\frac{\omega_0 m^*}{\hbar\sqrt{\Gamma}}\right)^{3/2} \exp\left\{-\pi\frac{K(\sqrt{\Gamma}) - E(\sqrt{\Gamma})}{E(\sqrt{\zeta})}]x+1[\right\} \tag{4}$$

with infinite sum Q:

$$Q = \sqrt{\frac{\pi}{2K(\sqrt{\zeta})}}\sum_{n=0}^{\infty}\left(\exp\left\{-\frac{n\pi[K(\sqrt{\Gamma}) - E(\sqrt{\Gamma})]}{E(\sqrt{\zeta})}\right\}\Phi\left(\sqrt{\eta(n+2\mu)}\right)\right) \tag{5}$$

and the following abbreviations::

$$\gamma = \frac{\omega_0}{e}\left(\frac{m^* c n_0 \epsilon_0 E_g}{2I}\right)^{1/2}, \qquad \Gamma = \frac{\gamma^2}{\gamma^2+1}, \qquad \zeta = \frac{1}{\gamma^2+1}$$
$$\eta = \frac{\pi^2}{2K(\sqrt{\zeta})E(\sqrt{\zeta})}, \qquad x = \frac{2}{\pi}\frac{E_g}{\hbar\omega_0}\frac{1}{\sqrt{\Gamma}}E(\sqrt{\zeta}), \qquad \mu =]x+1[-x \tag{6}$$

with γ: Keldysh parameter, ω_0: central laser frequency, m^*: effective electron mass, $]y[$: integer part of y, E_g: intrinsic material bandgap, c: speed of light in vacuum, ϵ_0: permittivity, n_0: refractive index, I: laser intensity, $\hbar$: Planck constant. Equations 4, 5 and 6 also include the Dawson Function

$$\Phi = \int_0^z \exp(y^2 - z^2)dy \tag{7}$$

and the elliptic integrals

$$K(k) = \int_0^{\pi/2} \frac{1}{\sqrt{1-k^2 sin^2(\phi)}}\,d\phi$$
$$E(k) = \int_0^{\pi/2} \sqrt{1-k^2 sin^2(\phi)}\,d\phi \tag{8}$$

The ionization rate caused by electron-electron collisions is modeled by the Drude-Theory which provides the following ionization rate[12,13]

$$W_{AI} = \frac{\sigma}{E_g}\rho(t) \tag{9}$$

where only the absorption cross section σ given by

$$\sigma = \frac{e^2}{c\epsilon_0 n_0 m^*}\frac{\tau_c}{1+\omega_0^2\tau_c^2} \tag{10}$$

with collision time

$$\tau_c = \frac{16\pi\epsilon_0^2\sqrt{m^* E_{\text{kin}}^3}}{\sqrt{2}e^4\rho} \tag{11}$$

depends on the laser frequency. Here the mean kinetic energy of the excited electrons is calculated by

$$E_{\text{kin}} = \frac{E_g}{10}\left(1+\frac{1}{4\gamma^2}\right) \tag{12}$$

2.2 Polychromatic algorithm

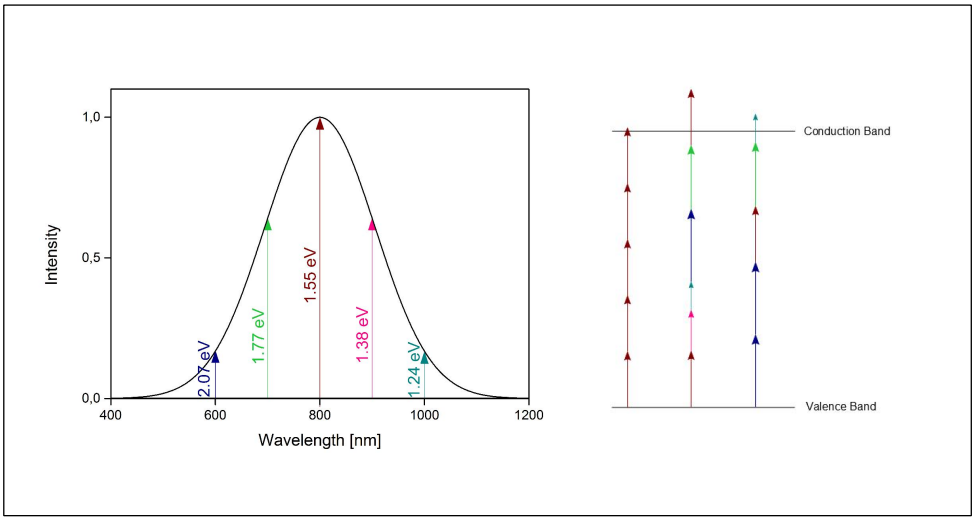

Figure 2. Schematic drawing of different excitation channels in the case of a broadband spectrum of a gaussian pulse of 5 fs pulse duration

The consideration of more than only the central frequency allows more than one excitation channel to evolve. A schematic drawing of possible excitation processes driven by several photons of different energy is sketched in figure 2. On the left hand side of the figure, a spectral intensity distribution for a gaussian pulse around a central wavelength of 800 nm is shown. On the right hand side different combinations of the marked frequencies from the left hand side are chosen to cross the gap between valence and conduction band. Generally, taking into account more than one frequency from the incoming pulse leads to a huge amount of possibilities for photon combinations that provide sufficient energy for the ionization of a valence electron. As the efficiency of this multiphoton excitation depends strongly on the number k of absorbed photons, a sufficiently broad spectrum might lead to a $k-1$ photon process, thus a much more efficient ionization of the irradiated material. The broader the spectrum of the incoming pulse, the higher the probability for high-energetic photons (compared to central frequency photons) to participate in the ionization process.
To compute the polychromatic behavior of the photoionization rate, the spectral intensity distribution obtained by fourier transformation of the temporal pulse shape as given in table 1 is interpreted as a probability distribution of different frequencies contained in the pulse around the central laser frequency ω_0. Thus, the spectral intensity

close to the central frequency is higher than for photons of distant frequencies independently of the pulse shape. After calculating the photon distribution, photons can be picked by a randomized procedure according to their spectral intensity distribution in a Monte-Carlo algorithm. This "photon lottery" is continued until the total photon energy exceeds the effective bandgap energy $\widetilde{E}_g$ which is the sum of the standard bandgap energy E_g and the ponderomotive energy of the free carrier. Hence, the termination condition for picking further photons reads

$$\sum_{i=1}^{k} \hbar\omega_i \geq \widetilde{E}_g, \qquad \widetilde{E}_g = E_g + \frac{e^2|E|^2}{4m_e\omega_0^2} \tag{13}$$

Here, only the central frequency ω_0 was used to approximate the ponderomotive shift of the bandgap. The number k of involved photons (multiphoton order) thereby strongly depends on the spectral width and consequently on the pulse duration and the temporal pulse shape.
Subsequently, the photoionization rate is calculated for each of the frequencies ω_i according to equation 4 and is normalized by dividing the sum of the calculated ionization rates by the number of the picked photons k to obtain an effective photoionization rate of this particular excitation channel:

$$W_{\mathrm{PI}}^{\mathrm{Ch}} = \frac{1}{k}\sum_{i=1}^{k} W_{\mathrm{PI}}(\omega_i) \tag{14}$$

As the selection of the photon frequencies is a statistical process, a repetition of the described steps is necessary to reach statistical safety. Hence, the described algorithm is repeated l times where l denotes the number of iterations in the algorithm. The required number of iterations to reach statistical safety strongly depends on the bandwidth of the spectrum. As the possibility to cover a multiphoton order transition wavelength increases for a broader spectrum, the number of required repetitions of the Monte-Carlo algorithm scales with the spectral width. Statistical safety is quantified by minimizing the standard error of the mean $SE(\overline{\Omega}) = \frac{\sigma}{\sqrt{N}}$ with mean $\overline{\Omega}$, number of picked photons N and standard deviation of a single pick $\sigma = \sqrt{\mathrm{Var}(\Omega)}$. The variance for a discrete random variable is thereby given by $\mathrm{Var}(\Omega) = \sum_{\omega\in A}(\omega-\mu)^2 S(\Omega=\omega)$ with expectation value $\mu = \sum_{\omega\in A}\omega S(\Omega=\omega)$, range of values A and probability function S. In practice, the number of iterations is increased until the standard error of the mean falls below 1. Finally, the effective polychromatic ionization rate results from summing and normalizing the effective ionization rates of the different excitation channels by

$$W_{\mathrm{PI}}^{\mathrm{Poly}} = \frac{1}{l}\sum_{j=1}^{l}\left(W_{\mathrm{PI}}^{\mathrm{Ch}}\right)_j \tag{15}$$

The total number of picked photons N is then given by

$$N = \sum_{j=1}^{l} k_j \tag{16}$$

Analogous to the procedure described above, the spectral width has to be considered in the computation of the avalanche ionization rate as well. To include the wavelengths contained in the laser pulse the absorption cross section σ is converted to

$$\sigma_{\mathrm{Poly}} = \frac{1}{N}\sum_{i=1}^{N}\sigma_i(\omega_i) \tag{17}$$

with σ_i representing the single-frequency cross section given in equation 10, which leads to an effective absorption cross section containing all photons that are involved in the ionization process.
The described methods can be used to solve the rate equation 3 to obtain the plasma density buildup induced by laser pulses of arbitrary spectral and temporal shape. To calculate the theoretical LIDT of the irradiated material, a critical value for the conduction band electron density ρ_{crit} as reported in[6] is used as a damage criterion. This threshold value can be derived by equating the plasma frequency $\omega_p = \sqrt{\rho e^2/m^*\epsilon_0}$ to the central laser frequency and thus follows to

$$\rho_{crit} = \frac{\epsilon_0 m^* \omega_0^2}{e^2} \tag{18}$$

For the case of many involved frequencies, the damage criterion has to be converted to

$$\rho_{crit}^{poly} = \frac{1}{N}\sum_{i=1}^{N}\rho_{crit}(\omega_i) \tag{19}$$

3. RESULTS

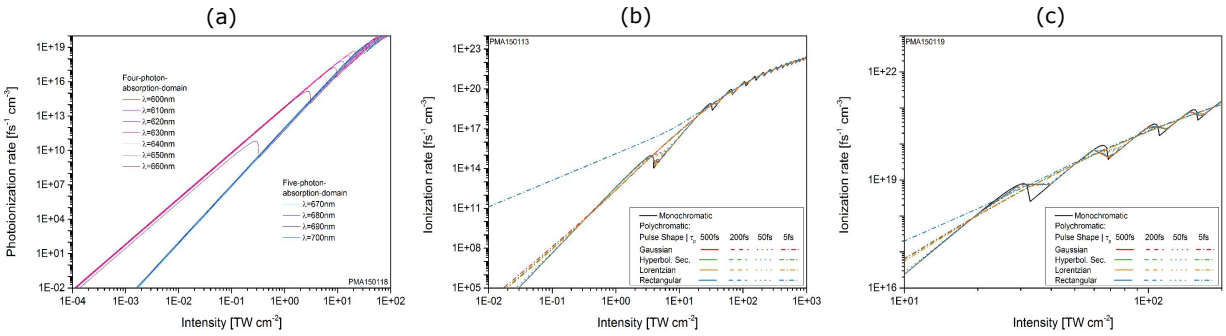

Figure 3. (a) Transition from four to five photon absorption domain in fused silica, (b) Comparison of mono- and polychromatic ionization rates for different temporal pulse shapes, (c) zoom in the region of interest

Using the methods presented above, the ionization of a dielectric material under irradiation with an ultrashort broadband laser pulse can be calculated. Results for fused silica are shown in figure 3(b). Material parameters used for the simulation can be found in table 2. The main differences between the monochromatic rate and the rates resulting from the polychromatic approach are the increased ionization rate for low intensities and the disappearance of the multiphoton order steps with decreasing pulse duration. Both differences can be traced back to the spectral width of the USP.

In figure 3(a) monochromatic ionization rates are shown for various wavelengths around the transition from four to five photon absorption domain. The significantly higher ionization probability for a four photon absorption process in the low intensity regime can be considered for an explanation for the increased rate of the polychromatic simulation. The growing number of different wavelengths contained in pulses with decreasing pulse durations opens up the possibility for further excitation channels. Consequently, with increasing spectral width the multiphoton order is reduced from k to $k-1$ with finite probability. As the photoionization rate is more efficient for $k-1$ than for k photons involved, the influence of photons with frequency $\omega > \omega_0$ shifts the curve in the direction of the lower order rates, even if the central frequency is closer to an $n \to n+1$ than an $n \to n-1$ transition.

Multiphoton order steps appear in the traditional Keldysh formalism every time the laser field is modifying the material bandgap by the DC Stark shift in such a way that the number of necessary photons to excite one electron from a bound state to a free state is increasing. Caused by the different photons contained in the polychromatic simulation these steps are smoothed out until they completely vanish at sufficient spectral width. This behavior is elucidated in figure 3(c) where the smoothing of the steps in the photoionization rate is illustrated for several pulse durations and temporal intensity profiles.

In figure 4 numerical results for wavelength dependent LIDT are presented for SiO_2 and TiO_2 irradiated with laser pulses of different temporal shapes and a pulse duration between $5 - 500\,\mathrm{fs}$. Numerical results obtained with the presented polychromatic approach are compared with monochromatic simulations. These results reveal that for pulse durations of a few hundreds of femtoseconds the spectral width of the incident laser pulses can be neglected because the polychromatic approach leads to the same results as the monochromatic calculation. For shorter pulses the spectral width is sufficient to allow more efficient ionization processes in the material which generally leads to a reduction of the theoretical damage threshold. The strongest influence can be observed for temporal pulse shapes with a larger c_{TBP}-factor while the smallest difference between the poly- and monochromatic simulation can be found for the lorentzian pulse shape due to the smallest time-bandwidth product.

Table 2. Material parameters for the dielectric materials used in the simulations

Material	Bandgap [eV]	Refractive index	relaxation time [fs]	red. electron mass [m_e]
SiO_2	7.5	1.45 @ 800 nm	220	0.635
TiO_2	3.4	2.48 @ 800 nm	300	0.3

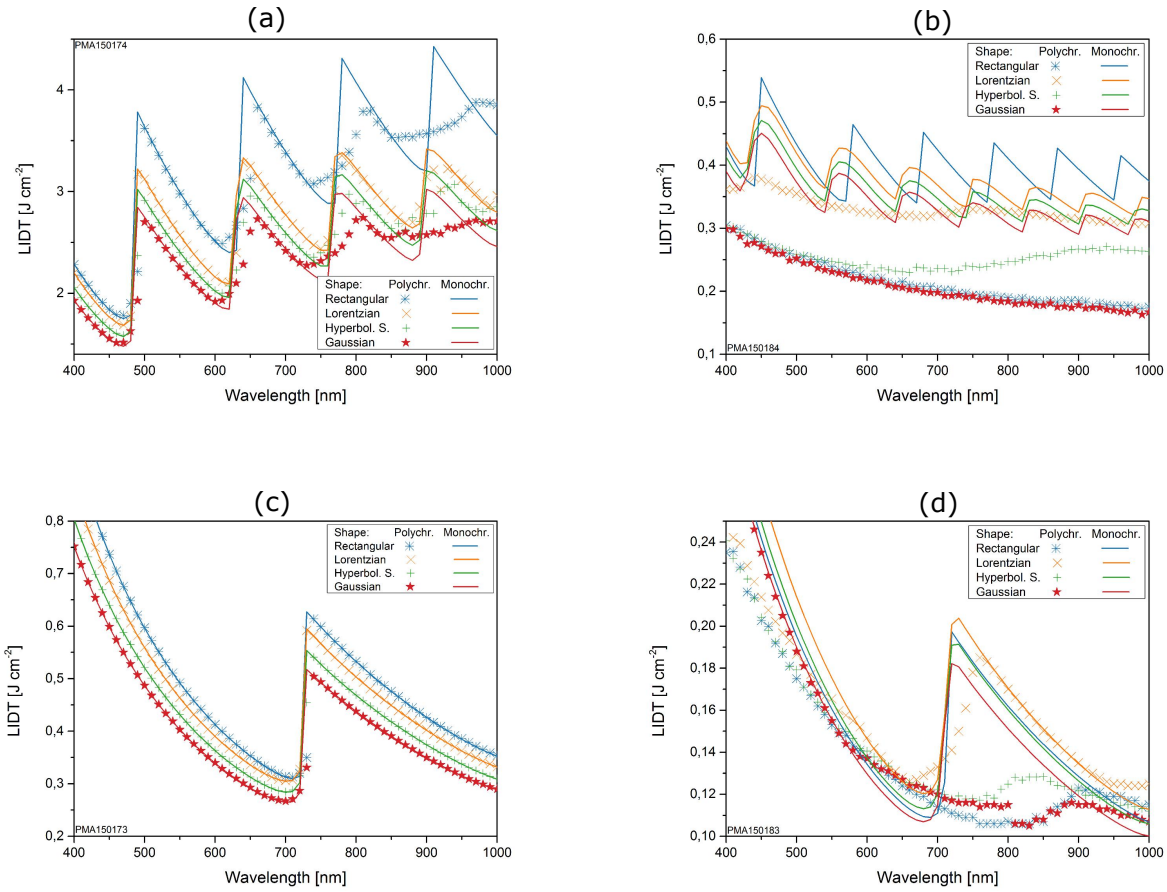

Figure 4. Wavelength dependent LIDT of (a) SiO_2, $\tau_p = 200\,\text{fs}$, (b) SiO_2, $\tau_p = 5\,\text{fs}$, (c) TiO_2, $\tau_p = 500\,\text{fs}$, (d) TiO_2, $\tau_p = 50\,\text{fs}$

As already found in the ionization rates, the steps in the wavelength dependent LIDT, resulting from a change of the multiphoton order, start to smooth out and disappear with decreasing pulse duration and increasing wavelength for the reasons already mentioned. Furthermore, a shift of these steps towards longer wavelengths can be observed.

4. SUMMARY

Numerical simulations considering the influence of the spectral width of USP during the ionization of dielectric solids demonstrate that neglecting the different spectral components generally leads to a miscalculation for pulse durations below a few hundreds of femtoseconds. The formation of further excitation channels induced by the spectral distribution yields a higher ionization rate especially in the low intensity regime leading to a reduced theoretical LIDT. The uncertainty of the multiphoton order during ionization leads to a smoothing of the steps

in the wavelength dependence of laser-induced damage caused by a change of the multiphoton order.
These results indicate that the spectral width of USP should be considered in accurate models of laser matter interaction especially in the case of pulse durations below $\approx 200\,fs$. Furthermore, the presented algorithm is not only suited to simulate the interaction of broadband USP with solid dielectrics but has also been successfully applied to the problem of two-pulse, two-color excitation of dielectric thin films.[14,15]

Acknowledgements

The authors thank the Ministry for Science and Culture of Lower Saxony and the Volkswagen Stiftung for the financial support of the research project "Hybride Numerische Optik" (contract no. ZN361).

REFERENCES

[1] B. C. Stuart, M. D. Feit, S. Herman, A. M. Rubenchik, B. W. Shore, and M. D. Perry, "Nanosecond-to-femtosecond laser-induced breakdown in dielectrics," *Phys. Rev. B* **53**(4), 1996.

[2] M. Mero, J. Liu, and W. Rudolph, "Scaling laws of femtosecond laser pulse induced breakdown in oxide films," *Phys. Rev. B* **71**(11), 2005.

[3] L. A. Emmert, M. Mero, and W. Rudolph, "Modeling the effect of native and laser-induced states on the dielectric breakdown of wide band gap optical materials by multiple subpicosecond laser pulses," *J. Appl. Phys.* **108**(4), 2010.

[4] J. R. Gulley, "Frequency dependence in the initiation of ultrafast laser-induced damage," in *Proc. SPIE*, **7842**, 2010.

[5] B. Rethfeld, "Unified model for the free-electron avalanche in laser-irradiated dielectrics," *Phys. Rev. Lett.* **92**(18), 2004.

[6] M. Jupé, L. Jensen, A. Melninkaitis, V. Sirutkaitis, and D. Ristau, "Calculations and experimental demonstration of multi-photon absorption governing fs laser-induced damage in titania," *Opt. Express* **17**(15), 2009.

[7] L. Gallais, D.-B. Douti, M. Commandré, G. Batavičiūtė, E. Pupka, M. Ščiuka, L. Smalakys, V. Sirutkaitis, and A. Melninkaitis, "Wavelength dependence of femtosecond laser-induced damage threshold of optical materials," *J. Appl. Phys.* **117**(22), 2015.

[8] L. V. Keldysh, "Ionization in the field of a strong electromagnetic wave," *Soviet Physics JETP* **20**(5), 1965.

[9] P. Martin, S. Guizard, P. Daguzan, G. Petite, P. D'Oliveira, P. Meynadier, and M. Perdrix, "Subpicosecond study of carrier trapping dynamics in wide-band-gap crystals," *Phys. Rev. B* **55**(9), 1997.

[10] A. V. Mitrofanov, A. J. Verhoef, E. E. Serebryannikov, J. Lumeau, L. Glebov, A. M. Zheltikov, and A. Baltuška, "Optical detection of attosecond ionization induced by a few-cycle laser field in a transparent dielectric material," *Phys. Rev. Lett.* **106**(14), 2011.

[11] B. G. Gorshkov, A. S. Epifanov, and A. A. Manenkov, "The relative role of impact and multiphoton ionization mechanisms in laser induced damage of transparent dielectrics," *Laser Induced Damage in Optical Materials: 1978* , 1979.

[12] M. D. Feit and J. J. A. Fleck, "Effect of refraction on spot-size dependence of laser-induced breakdown," *Appl. Phys. Lett.* **24**(4), pp. 169 – 172, 1974.

[13] K. Starke, D. Ristau, H. Welling, T. V. Amotchkina, M. Trubetskov, A. A. Tikhonravov, and A. S. Chirkin, "Investigations in the non-linear behavior of dielectric coatings by using ultrashort pulses," in *Proc. SPIE*, **5273**, 2004.

[14] M. Gyamfi, P. Jürgens, M. Mende, L. Jensen, and D. Ristau, "Dual-wavelength ultra-short pulse laser damage testing," in *Proc. SPIE*, **9237**, 2014.

[15] M. Gyamfi, P. Jürgens, L. Jensen, and D. Ristau, "Delay dependency of two-pulse femtosecond laser damage," in *Proc. SPIE*, **9632**, 2015.